Available online at www.sciencedirect.com
ScienceDirect
Journal of Computational Physics 227 (2008) 9008–9020
JOURNAL OF COMPUTATIONAL PHYSICS
www.elsevier.com/locate/jcp

Resolution requirements for aero-optical simulations

Ali Mani [a,*], Meng Wang [b], Parviz Moin [a]

[a] Department of Mechanical Engineering, Stanford University, CA 94305, United States
[b] Department of Aerospace and Mechanical Engineering, University of Notre Dame, Notre Dame, IN 46556, United States

Received 11 October 2007; received in revised form 1 February 2008; accepted 5 February 2008
Available online 23 February 2008

Abstract

Analytical criteria are developed to estimate the error of aero-optical computations due to inadequate spatial resolution of refractive index fields in high Reynolds number flow simulations. The unresolved turbulence structures are assumed to be locally isotropic and at low turbulent Mach number. Based on the Kolmogorov spectrum for the unresolved structures, the computational error of the optical path length is estimated and linked to the resulting error in the computed far-field optical irradiance. It is shown that in the high Reynolds number limit, for a given geometry and Mach number, the spatial resolution required to capture aero-optics within a pre-specified error margin does not scale with Reynolds number. In typical aero-optical applications this resolution requirement is much lower than the resolution required for direct numerical simulation, and therefore, a typical large-eddy simulation can capture the aero-optical effects. The analysis is extended to complex turbulent flow simulations in which non-uniform grid spacings are used to better resolve the local turbulence structures. As a demonstration, the analysis is used to estimate the error of aero-optical computation for an optical beam passing through turbulent wake of flow over a cylinder.
© 2008 Elsevier Inc. All rights reserved.

Keywords: Aero-optics; Spatial resolution; Large-eddy simulation; Computational error; Compressible turbulent flow

1. Introduction

In this paper we propose analytical criteria to estimate the spatial resolution required for aero-optical simulations. In such simulations the refractive index field, which is directly related to the fluctuating density field, is obtained from a time dependent flow simulation such as large-eddy simulation (LES). The minimum requirement for flow-field resolution that allows for accurate predictions of optical distortions is the focus of this study. In this section, the general framework of aero-optical problems is introduced, followed by a brief review of aero-optical studies and different computational approaches. The analysis is introduced in Section 2 by considering simplified models, such as homogeneous turbulence resolved on a uniform mesh. In Section 3 further details regarding the underlying assumptions of the analysis are discussed, and its extension to more complex cases is presented. A numerical example is presented in Section 5 where LES of flow over a circular

* Corresponding author. Tel.: +1 650 723 9548; fax: +1 650 725 3525.
E-mail address: alimani@stanford.edu (A. Mani).

0021-9991/$ - see front matter © 2008 Elsevier Inc. All rights reserved.
doi:10.1016/j.jcp.2008.02.014

cylinder at $Re = 3900$ and $M = 0.4$ is considered for aero-optical computations, and the error due to lack of resolution is compared with the predicted error by the proposed analysis.

1.1. Aero-optical framework

The field of aero-optics generally focuses on the far-field distortions of optical beams due to compressible turbulence near optical apertures [1]. The flows of interest include boundary layers, wakes and cavity flows, typically associated with flight through the atmosphere. Although the depth of turbulence in a typical aero-optical field is not more than a few optical aperture diameters, density fluctuations in these flows can cause wavefront distortions of the order of a few optical wavelengths [2,3]. Such initial distortions reduce the coherence of the beams, so that by the time they arrive at the receivers, they have much lower intensities and are more dispersed compared to undistorted beams.

An optical beam under such conditions experiences two regimes of propagation: first, propagation through the turbulence near the optical device, where density fluctuations are significant and of relatively high frequency/wavenumber and second, propagation through the atmosphere (see Fig. 1). In the first region, since the distance is very short and the optical wavelength is much smaller than the flow structures, the ray optics assumptions are valid. Furthermore, due to the fact that the refractive index variations are very small, passing through the first region only causes phase errors in the beam. In other words, scattering and change in the optical wave amplitude can be ignored in this region. As in Fig. 1, considering z as direction of optical propagation, one can express this phase distortion as [1,4]

$$U(x,y,z_1) = U(x,y,z_0)\exp\left[\frac{-2\pi \mathrm{j}\mathcal{L}(x,y)}{\lambda}\right], \tag{1}$$

$$\mathcal{L}(x,y) = \int_{z_0}^{z_1} n(x,y,z)\mathrm{d}z, \tag{2}$$

where U is the electromagnetic field, λ is the optical wavelength, $\mathrm{j} = \sqrt{-1}$, n represents the refractive index, z_0 and z_1 represent the boundaries of the turbulent regime (first region), and $\mathcal{L}$ is referred to as the optical path length (OPL) and represents the time of travel between z_0 and z_1 for individual rays. Since the fluctuations in the index of refraction are of small amplitude, $|n-1| \ll 1$, it can be shown that variations of $\mathcal{L}$ with x and y represent wavefront distortions at z_1 [4].

After the beam passes through the turbulent regime, it travels a long distance to the receiver. Mani et al. [5] have provided a useful description of far-field propagation in which the initial wavefront aberrations and diffraction effects are linked separately to the far-field optical distortions. It should be noted that the problem of distortion due to atmospheric turbulence can generally be corrected using adaptive optics because the

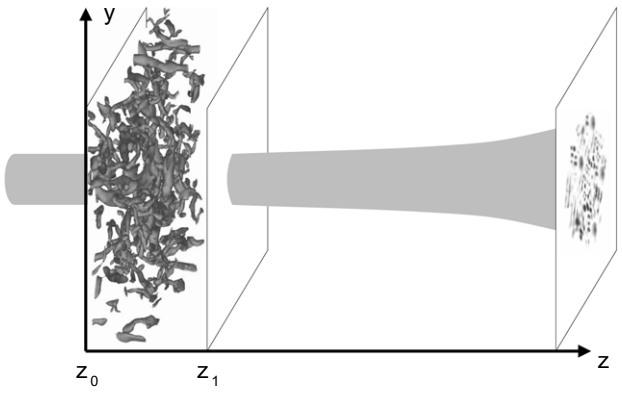

Fig. 1. Schematic of aero-optical distortions and a typical computational setup.

refractive index field involves larger spatio-temporal scales. In the present analysis we assume free-space propagation to the far-field.

1.2. Computational approaches to aero-optics

In contrast to the problem of wave propagation in a turbulent atmosphere, which has been tackled primarily with the application of wavefront sensors and deformable correction mirrors, the aero-optical distortions usually take place at spatial and temporal frequencies which are orders of magnitude higher than the capabilities of current correction technologies [6,7]. The high frequency of the problem also makes it technically difficult and expensive to investigate experimentally. Since the late 1980's, numerical studies of aero-optical phenomena, which allow for the probing of flows and optical fields in greater detail, have emerged as a valuable tool to complement experiments.

Due to lack of computational power, earlier computations were typically based on Reynolds-averaged Navier–Stokes (RANS) calculations with a turbulence model, such as the k–ε model [8,9]. However, since aero-optics is highly dependent on fluctuations in the turbulent density field, an accurate representation of aero-optical distortions with a RANS simulation alone is not possible. Optical modeling is generally required in addition to turbulence modeling to represent the optical distortions. These types of approaches involve adjustable model parameters which are flow-regime dependent and must often be tuned for a given flow configuration.

Truman [10] and Truman and Lee [11] performed one of the first computational studies of aero-optical distortions using direct numerical simulations (DNS) of a homogeneous shear flow as well as a turbulent channel flow. They used a passive scalar field in an incompressible flow to model fluctuations of the refractive index field. Truman [10] found that large turbulence structures provided the dominant contributions to the wavefront distortions.

Since DNS of a realistic flow is prohibitively expensive, LES is of major recent interest for aero-optical computations. LES is capable of capturing a range of flow structures, from large-scale motions down to the scale comparable to the mesh spacing, while the effect of unresolved features is modeled. LES has been used for aero-optical computations in various flow configurations, from simple shear [4,12,13] and wake [3] flows to flows around complex objects, such as the fuselage of an aircraft [2].

In most of the previous LES-based studies, the grid resolution requirement for accurate representation of aero-optical effects have not been considered. In addition, in order to provide robustness, most studies have used dissipative numerical schemes, which have been shown to artificially damp resolvable small scales of the flow [14]. In these simulations, it has been implicitly assumed that sub-grid scales and artificially damped resolved small-scale features of the flow are optically unimportant. Although these simulations may capture low order flow statistics, this does not necessarily guarantee that the aero-optical effects of the flow can be provided with the same resolution. Without a resolution criterion grid convergence studies are needed to ensure the satisfactory resolution of the aero-optical effects (see, for example, Tromeur et al. [4]).

Although the resolution requirements for computing turbulent flows and their Reynolds number dependence are reasonably established, there is not much information in the literature regarding the resolution requirements for aero-optical simulations. This motivated us to perform an analysis on this issue to provide a rule-of-thumb estimate of grid spacing required for such simulations. As will be observed in Section 2, parameters such as the optical wavelength and the free stream refractive index, which do not play a role in hydrodynamics, are very important in determining optically important scales.

Another area of potential interest in this research is optical sub-grid-scale modeling for aero-optical simulations. Since LES does not resolve flow scales smaller than grid spacing, the potential need for an optical sub-grid-scale model (in addition to the flow sub-gird model) has become a topic under consideration. Using that type of approach, the optical effects of unresolved flow structures will be mathematically modeled. Nevertheless, it is useful to first examine the cost of resolving all of the relevant scales for aero-optical computations and how it scales with the Reynolds number as the Reynolds number becomes very high. Our analysis determines the resolution required for accurately capturing the aero-optical distortions. By comparing this resolution to the resolution required for flow simulation, we can determine whether to use an optical sub-grid model or resolve the optically active scales without resorting to such modeling.

2. Analysis

In this section, the influence of inadequate spatial resolution on the error of aero-optical computations is analyzed. The analysis involves three major steps: first, an error measure for aero-optical computations is established and linked to the error in the computed OPL. Based on this error measure an accuracy criterion is introduced; second, the wavenumber spectrum of the OPL is linked to the spectrum of the index of refraction field and, thus, to the density and the pressure field; third, by considering a Kolmogorov spectrum for the unresolved flow, the error of aero-optical computation due to unresolved flow is estimated.

In this section we make simplifying assumptions such as homogeneity and isotropy of turbulence and uniform grid spacing. Since some of these assumptions limit the applicability of the results for practical problems, a modified analysis applicable to complex cases is introduced in Section 3.

2.1. Step 1: error measure for aero-optical computations

To begin the analysis, we start with the beam introduced in Section 1.1. Eq. (1) describes the electromagnetic field after the beam passes the turbulent region. Since $U(x,y,z_0)$, the field at the aperture, is analytically known, the only error in computation of electromagnetic field after the beam passes the turbulence region can be caused by computational errors in $\mathcal{L}$. One can write

$$\mathcal{L} = \mathcal{L}_n + \mathcal{L}_e, \tag{3}$$

where subscripts n and e represent the numerical value and the error value due to unresolved flow, respectively. Due to linearity, it is clear that a relation similar to Eq. (2) exists between $\mathcal{L}_e$ and the unresolved refractive index field n_e. Substituting Eq. (3) into Eq. (1) and using a Taylor expansion around $\mathcal{L} = \mathcal{L}_n$ result in

$$U(x,y,z_1) = U(x,y,z_0)\exp\left[-\frac{2\pi \mathrm{j}}{\lambda}\mathcal{L}_n\right] - \left(\frac{2\pi j}{\lambda}\mathcal{L}_e\right)U(x,y,z_0)\exp\left[-\frac{2\pi \mathrm{j}}{\lambda}\mathcal{L}_n\right] + \mathcal{O}\left(\mathcal{L}_e^2/\lambda^2\right). \tag{4}$$

Note that in aero-optical computations, distances far beyond z_1, called the far-field, are the locations where U must be accurately computed. Fourier optics methods can compute the wave propagation after z_1 almost without additional errors. According to Eq. (4), the beam properties at z_1 are written as the superposition of two beams; the first term on the right hand side represents the computed beam, and the remaining terms represent the error beam (U_e). Both of these beams propagate in the far-field according to the wave equation, and their energy remains constant. Therefore, the far-field computations will be accurate if, and only if, at location z_1 the error beam has much less energy than the computed beam. Henceforth, a simple criterion to check the accuracy of aero-optical computations can be based on this energy ratio. If the ratio is smaller than a threshold, ξ, for example 5%, then one can assume that the resolution of the flow simulation is adequate to capture the aero-optical effects. From Eq. (4) this energy ratio is,

$$\left(\frac{2\pi}{\lambda}\right)^2 \int\int \mathcal{I}(x,y)\mathcal{L}_e(x,y)^2 \mathrm{d}x\,\mathrm{d}y < \xi, \tag{5}$$

where $\mathcal{I} = |U(x,y,z_0)|^2 / \int\int |U(x,y,z_0)|^2 \mathrm{d}x\,\mathrm{d}y$ is the normalized aperture intensity profile, and the integration domain is composed of all x and y locations corresponding to the beam's aperture. In most applications the aperture profile is either a smooth function or a top-hat function. To further simplify Eq. (5) one can decompose the integration domain into some small areas over which $\mathcal{I}$ can be considered constant. Given the small correlation length scale of $\mathcal{L}_e$, compared to the size of these areas, one can replace $\mathcal{L}_e^2$ with its ensemble average based on the ergodic assumption. Recombining the integrals over the smaller domains into one integral results in

$$\int\int \mathcal{I}\mathcal{L}_e^2 \mathrm{d}x\,\mathrm{d}y \simeq \int\int \mathcal{I}\overline{\mathcal{L}_e^2}\mathrm{d}x\,\mathrm{d}y, \tag{6}$$

where the over-line indicates the ensemble average. If the unresolved flow is assumed statistically homogeneous in x and y, $\overline{\mathcal{L}_e^2}$ does not depend on x and y. Noting that $\int\int \mathcal{I}\mathrm{d}x\,\mathrm{d}y = 1$, Eq. (5) can be simplified to

$$\left(\frac{2\pi}{\lambda}\right)^2 \overline{\mathcal{L}_e^2} < \xi. \tag{7}$$

$(2\pi/\lambda)^2\overline{\mathcal{L}_e^2}$ is an error measure for aero-optical computations, and Eq. (7) is the proposed criterion for accuracy of aero-optical computations.

2.2. Step 2: OPL spectrum in terms of the pressure spectrum

In order to assess the adequacy of the flow resolution, we need to link $\overline{\mathcal{L}_e^2}$ to the resolution of the flow simulation. At this step, we first seek a relationship between correlation functions of the OPL error, $\mathcal{R}_{\mathcal{L}_e}(x,y) = \overline{\mathcal{L}_e(x'+x,y'+y)\mathcal{L}_e(x',y')}$, and that of the unresolved index of refraction field, $\mathcal{R}_{n_e}(x,y,z)$. In Appendix A it is shown that

$$\mathcal{R}_{\mathcal{L}_e}(x,y) \simeq \Delta z \int_{-\infty}^{+\infty} \mathcal{R}_{n_e}(x,y,z)\mathrm{d}z, \tag{8}$$

where $\Delta z = z_1 - z_0$. In deriving Eq. (8) it has been assumed that the correlation length of the unresolved flow is much smaller than the aperture size and depth of turbulence over which the optical beam propagates. Using Eq. (8) a relationship between the two-dimensional spectrum of the wavefront error, $\widehat{\mathcal{R}_{\mathcal{L}_e}}(k_x,k_y)$, and the three-dimensional spectrum of the unresolved refractive index field, $\widehat{\mathcal{R}_{n_e}}(k_x,k_y,k_z)$, can be obtained

$$\begin{aligned}\widehat{\mathcal{R}_{\mathcal{L}_e}}(k_x,k_y) &= \frac{1}{(2\pi)^2}\int\int \mathcal{R}_{\mathcal{L}_e}(x,y)\exp\left[\mathrm{j}(k_x x + k_y y)\right]\mathrm{d}x\,\mathrm{d}y \\ &= \frac{\Delta z}{(2\pi)^2}\int\int\int \mathcal{R}_{n_e}(x,y,z)\exp\left[\mathrm{j}(k_x x + k_y y)\right]\mathrm{d}x\,\mathrm{d}y\,\mathrm{d}z = (2\pi\Delta z)\widehat{\mathcal{R}_{n_e}}(k_x,k_y,0).\end{aligned} \tag{9}$$

According to the Gladstone–Dale law, the refractive index field is a function of density [15]. Also assuming a high Reynolds number flow with small variation of the sound speed, one can relate density fluctuations to pressure fluctuations:

$$n = 1 + G(\lambda)\rho, \tag{10}$$

$$p - p_0 = c_0^2(\rho - \rho_0), \tag{11}$$

where ρ is the fluid density, G is the Gladstone–Dale constant, p represents the pressure field, c is the speed of sound, and subscript 0 represents values at the free stream. Therefore, spectral information regarding the pressure field can be linked to the spectrum of the refractive index field. Because Eqs. (10) and (11) are linear, similar relations such as Eqs. (10) and (11) exist between the unresolved quantities (i.e. $n_e = \frac{G}{c_0^2}p_e$). Rewriting Eq. (9) based on pressure spectrum results in

$$\widehat{\mathcal{R}_{\mathcal{L}_e}}(k_x,k_y) = (2\pi\Delta z)\left(\frac{G(\lambda)}{c_0^2}\right)^2 \widehat{\mathcal{R}_{p_e}}(k_x,k_y,0). \tag{12}$$

2.3. Step 3: Kolmogorov hypothesis for unresolved flow

There are published results concerning pressure fluctuations in incompressible turbulent flow fields (see for example [16–18]), which can be used to estimate the pressure spectrum here given the low turbulence Mach number. It should be noted that in the literature it has been less common to report the spectrum in the three-dimensional form ($\widehat{\mathcal{R}_p}(k_x,k_y,k_z)$). Instead, the one-dimensional energy spectrum $E_p(k)$ is frequently reported. $E_p(k)$ is the integral of the three-dimensional pressure spectrum $\widehat{\mathcal{R}_p}(k_x,k_y,k_z)$ over spherical shells of constant k. For an isotropic field, the two spectra are related by

$$\widehat{\mathcal{R}_p}(k_x,k_y,k_z) = E_p(|\,k\,|)/(4\pi\,|\,k\,|^2), \tag{13}$$

where $|\,k\,| = (k_x^2 + k_y^2 + k_z^2)^{1/2}$. According to the Kolmogorov hypothesis, the pressure energy spectrum in the inertial range of a locally isotropic flow is [17]

$$E_p(k) = B_p \rho_0^2 \epsilon^{4/3} k^{-7/3}, \tag{14}$$

where B_p is a constant of order unity and ϵ is the turbulent dissipation rate. Gotoh and Fukayama [18] estimated B_p to be 8.0 ± 0.5 using a DNS of isotropic turbulence. Next, we assume that the flow has been simulated using LES on a uniform grid with a cut-off wave-number k_c. This cut-off wavenumber is usually in the inertial range and is smaller than the wavenumber associated with Kolmogorov length scale, $k_\eta = 2\pi/\eta$. Therefore, assuming a "perfect" LES in the sense that it captures the flow at wave-numbers smaller than k_c, a simple spectrum for the unresolved pressure field would be (note Eq. (14))

$$E_{p_e}(k) = \begin{cases} B_p \rho_0^2 \epsilon^{4/3} k^{-7/3}, & k_c \leqslant k \leqslant k_\eta, \\ 0, & k > k_\eta \text{ or } k < k_c. \end{cases} \tag{15}$$

Since the spectrum after k_η has an exponential decay, it is simply ignored. By combining Eqs. (12), (13) and (15) the spectrum of $\mathcal{L}_e$ is obtained

$$\widehat{\mathcal{R}_{\mathcal{L}_e}}(k_x, k_y) = \frac{B_p \Delta z (n_0 - 1)^2}{2 c_0^4} \epsilon^{4/3} \mid k \mid^{(-7/3-2)}, k_c \leqslant k \leqslant k_\eta, \tag{16}$$

where $\mid k \mid = (k_x^2 + k_y^2)^{1/2}$. By integrating Eq. (16) over all wave-numbers, we can calculate the mean squared error of the computed wavefront:

$$\overline{\mathcal{L}_e^2} = \frac{3\pi B_p}{7} \left[\frac{(n_0 - 1)^2 \epsilon^{4/3}}{c_0^4} \right] \left[\left(\frac{l_c}{2\pi} \right)^{7/3} - \left(\frac{\eta}{2\pi} \right)^{7/3} \right] \Delta z, \tag{17}$$

where l_c is the grid resolution equal to $2\pi/k_c$. In the case of a very high Reynolds number, η becomes very small and can be ignored,

$$\overline{\mathcal{L}_e^2} = \frac{3\pi B_p}{7} \left[\frac{(n_0 - 1)^2 \epsilon^{4/3}}{c_0^4} \right] \left(\frac{l_c}{2\pi} \right)^{7/3} \Delta z. \tag{18}$$

By substituting Eq. (18) into Eq. (7) we obtain the criterion for checking the adequacy of the LES resolution:

$$\frac{12\pi^3 B_p}{7\lambda^2} \left[\frac{(n_0 - 1)^2 \epsilon^{4/3}}{c_0^4} \right] \left(\frac{l_c}{2\pi} \right)^{7/3} \Delta z < \xi. \tag{19}$$

2.4. Dependence on flow parameters

Eq. (19) is the fundamental result of this paper. For a compressible turbulence with parameters ϵ, c_0 and n_0, this equation determines the length scale that should be resolved in order to have accurate aero-optical computations with optical wavelength λ. Some of the interesting consequences of this result are discussed below.

1. In the high Reynolds number limit, the resolution requirement does not scale with Reynolds number. Although the hydrodynamic simulations require sub-grid scale models at high Reynolds numbers, we can avoid additional sub-grid modeling for aero-optics by resolving the critical scales given by Eq. (19).
2. For a flow with a characteristic length scale l and a characteristic velocity u, ϵ can be approximated as u^3/l. Therefore, Eq. (19) can be rewritten in the form

$$l_c \sim \frac{\xi^{3/7}}{M^{12/7}(n_0 - 1)^{6/7}} \frac{\lambda^{6/7} l^{4/7}}{\Delta z^{3/7}}, \tag{20}$$

where M is the characteristic turbulent Mach number of the flow (u/c_0). In this form, the required resolution is written as a function of the non-dimensional parameters, M, ξ and n_0, and three length scales, l, λ and Δz. According to this description, the important flow parameters are the turbulence length scale and the turbulent Mach number; the important optical parameters are the characteristic refractive index and optical wavelength; the important geometric parameter is the depth of the turbulence field.

3. In a typical aero-optical setup one can have, for example, $l \sim 1m$, $\Delta z \sim 1m$, $\lambda \sim 1\mu m$, $M \sim 0.4$, $(n_0 - 1) \sim 10^{-4}$ and $\xi \sim 5\%$. Based on these parameters, assuming $B_p = 8.5$ from Ref. [18] Eq. (19) predicts the value of l_c to be about 1.2 cm. Assuming that resolving such wavelengths requires grid spacing of 6 mm (based on Nyquist criterion), the required number of grid points in each direction would be approximately 170. In other words, with only five million grid points, the aero-optics of this flow can be captured accurately. Such a requirement can be readily met by a moderate parallel computing facility. Moreover, it should be noted that such a resolution is similar to practical LES resolutions. As a result, under typical flow conditions, resolving optically relevant scales do not need considerable aditional cost compared to that of LES.
4. It should be noted that under extreme conditions the resolution requirements for capturing optical effects may be close to that of DNS. For example, one can imagine a case where the optical device uses an extremely small wavelength (much smaller than $10^{-6}m$) so that acceptable $\overline{\mathcal{L}_e^2}$ becomes very small (see Eq. (7)). In such a case if Reynolds number is not very high, Eq. (17) can lead to l_c values very close to η. Under such conditions the approximation of Eq. (18) which ignores the η term is invalid and leads to very conservative estimates for l_c.

3. Extension to complex simulations

The procedure for obtaining Eq. (19) was based on the following assumptions: (1) smooth or piecewise smooth aperture optical intensity profile; (2) small correlation length of unresolved flow compared to the aperture size; (3) small correlation length of unresolved flow compared to the turbulence depth; (4) high Reynolds number flow; (5) isotropic unresolved scales; (6) uniform grid resolution and (7) homogeneous flow statistics and small variation of the sound speed (low turbulence Mach number).

The correlation length scale of unresolved flow is typically of order of the grid spacing l_c. Therefore, if the LES grid is such that the aperture intensity profile and the geometry of the flow are well resolved, assumptions 1-3 will be satisfied. Since the small structures of high Reynolds number flows are isotropic, small grid spacing automatically guarantees the fifth assumption. In summary, assumptions 1–5 will be satisfied if

$$l_c \ll l_{\text{geometry}}, l_{\text{aperture}}. \tag{21}$$

This relation is usually satisfied for practical aero-optical flows and typical LES resolutions. As a result, assumptions 6 and 7 are the only ones that limit the applicability of the criterion developed, Eq. (19). In this section, we modify the preceding analysis in order to relax conditions 6 and 7 and extend the criterion to more practical flows. Nevertheless, even without modifications, Eq. (19) can still be used as a rule-of-thumb estimate of the adequacy of LES resolution. In that case, averaged values of l_c and ϵ can be used.

To extend the analysis to practical flows, we first assume that the flow statistics and grid resolution vary in the z direction only. In this case Eq. (7) is still valid, and it is only necessary to modify Eq. (18). One can decompose the flow domain in z direction into several sub-intervals such that the flow statistics and grid resolution are almost constant in each sub-interval. By decomposing $[z_0, z_1]$ into $[s_0, s_1] \cup [s_1, s_2] \cup [s_2, s_3]$, …, $[s_{n-1}, s_n]$ $(z_0 = s_0 \ll s_1 \ll s_2 \cdots \ll s_n = z_1)$, one can rewrite Eq. (2) in the following form,

$$\mathcal{L}_e = \int_{s_0}^{s_1} n_e \mathrm{d}z + \int_{s_1}^{s_2} n_e \mathrm{d}z + \cdots = \mathcal{L}_{e1} + \mathcal{L}_{e2} + \cdots + \mathcal{L}_{en}, \tag{22}$$

where $\mathcal{L}_{ei}$ ($i = 1$ to n) is the OPL error of the ith interval. $\overline{\mathcal{L}_e^2}$ can then be written as

$$\overline{\mathcal{L}_e^2} = \sum_{i=1}^{n} \overline{\mathcal{L}_{ei}^2} + \sum_{i \neq j} \overline{\mathcal{L}_{ei}\mathcal{L}_{ej}}.$$

The second summation is the correlation between sub-integrals of n_e corresponding to different sub-intervals. It is reasonable to assume that each sub-interval is well resolved such that the correlation length scale of n_e, which is of order l_c, is much smaller than the size of the local sub-interval; in other words we can assume that $\mathcal{L}_{ei}$ is uncorrelated with $\mathcal{L}_{ej}$ for $i \neq j$, and the ensemble average of their product is zero. Neglecting the second summation in Eq. (3) and using Eq. (18) to estimate $\overline{\mathcal{L}_{ei}^2}$ based on local parameters result in

$$\overline{\mathcal{L}_e^2} \simeq \frac{3\pi B_p}{7}\sum_{i=1}^{n}\left[\frac{(n_i-1)^2\epsilon_i^{4/3}}{c_i^4}\right]\left(\frac{l_{ci}}{2\pi}\right)^{7/3}(s_i-s_{i-1}) \simeq \frac{3\pi B_p}{7}\int_{z_0}^{z_1}\left[\frac{(\overline{n(z)}-1)^2\epsilon(z)^{4/3}}{\overline{c(z)}^4}\right]\left(\frac{l_c(z)}{2\pi}\right)^{7/3}\mathrm{d}z, \tag{23}$$

where $l_c(z)$ is a measure of the local resolution and is related to local grid spacing and discretization scheme used in CFD. Considering the capabilities of current LES methods, it is reasonable to estimate l_c based on the maximum value of grid spacing ($l_c \simeq 2\max\{\delta x, \delta y, \delta z\}$). By substituting Eq. (23) into Eq. (7) a more general version of the criterion can be obtained

$$\frac{12\pi^3 B_p}{7\lambda^2}\int_{z_0}^{z_1}\left[\frac{(\overline{n(z)}-1)^2\epsilon(z)^{4/3}}{\overline{c(z)}^4}\right]\left(\frac{l_c(z)}{2\pi}\right)^{7/3}\mathrm{d}z < \xi. \tag{24}$$

The analysis can be extended even further to cases where the flow and grid are not homogeneous in all directions. In this case, Eq. (5) cannot be simplified to the form of Eq. (7). However, assuming that the grid spacing in LES is much smaller than the length scale of inhomogeneity of flow statistics, Eq. (6) is still valid. Also, $\overline{\mathcal{L}_e^2}$ can be estimated by Eq. (23). Substituting Eq. (23) into Eq. (6) and then Eq. (5) leads to

$$\frac{12\pi^3 B_p}{7\lambda^2}\int\int_{\mathcal{I}}\int_{z_0}^{z_1}\left[\frac{(\bar{n}-1)^2\epsilon^{4/3}}{\bar{c}^4}\right]\left(\frac{l_c}{2\pi}\right)^{7/3}\mathrm{d}z\,\mathrm{d}y\,\mathrm{d}x < \xi, \tag{25}$$

where the integration domain in x-y plane is the same as the aperture. Eq. (25) is the most general form of the criterion. Recalling from Section 2.1, ξ is the threshold error and the left hand side of Eq. (25) is the error estimate of the computed electromagnetic field in the far-field (L_2 norm squared)

$$\frac{\int\int\overline{|U_e|^2}\mathrm{d}x\,\mathrm{d}y}{\int\int|U|^2\mathrm{d}x\,\mathrm{d}y} \simeq \frac{12\pi^3 B_p}{7\lambda^2}\int\int_{\mathcal{I}}\int_{z_0}^{z_1}\left[\frac{(\bar{n}-1)^2\epsilon^{4/3}}{\bar{c}^4}\right]\left(\frac{l_c}{2\pi}\right)^{7/3}\mathrm{d}z\,\mathrm{d}y\,\mathrm{d}x, \tag{26}$$

where U_e is the difference between the exact electromagnetic field and the one computed from coarse representation of the flow. If the criterion given by Eq. (25) is satisfied one can be assured that the flow resolution is adequate for capturing aero-optical effects within the pre-specified error margin. Based on the analysis Eq. (25) is valid if

1. the flow is at high Reynolds number;
2. the fields of $\bar{n}$, ϵ, $\bar{c}$, l_c and $\mathcal{I}$ are well resolved such that the length scale of inhomogeneity of these fields are much larger than the local grid spacings.

The second condition enables us to decompose the domain into sub-domains where we can apply the result of the homogeneous analysis (Eq. (19)). These new conditions are very likely to be satisfied in a typical LES. It should be noted that, to link the index of refraction field to pressure filed via Eqs. (10) and (11), we have implicitly assumed that unresolved pressure fluctuations are correlated to unresolved density fluctuations through the local ensemble-averaged speed of sound. This assumption is not valid if fluctuations of the Mach number are not small. However, since in error analysis, only the order of magnitude of the error is important this assumption can still be used as long as the unresolved turbulence is at low Mach number, even if the flow Mach number is not small.

4. Discussion

The analytical results presented above can be used for grid design in practical simulations. For a given aero-optics problem, once the flow and optical setup is known, one can perform a RANS simulation of the flow, which is computationally inexpensive, and obtain an estimate of the flow statistics such as ϵ, $\bar{c}$ and $\bar{n}$. Having a candidate grid for an aero-optical simulation, we can obtain the function $l_c(x, y, z)$ based on the local resolution of the grid. If l_c satisfies the condition given by Eq. (25) (which reduces to Eq. (24) or Eq. (19) for simpler cases) for a given aero-optical parameters, one can be assured that the grid has adequate resolution for the aero-optical computation. Based on this criterion we can also compare aero-optical errors of different grids and select the optimal grid for the simulation.

It should be noted that if the error of a given aero-optical simulation based on the introduced measure is ξ_0 (squared L_2 norm error), then according to Eq. (7), $\mathcal{L}_e$ is of order $\lambda\sqrt{\xi_0}$. In other words, while the energy of the error is of order ξ_0 the computational error of the electromagnetic field and the optical irradiance (due to unresolved structures) is of order $\sqrt{\xi_0} \sim \mathcal{L}_e/\lambda$ (cf. Eq. (4)). However, in most aero-optical applications we are interested in the ensemble-averaged far-field irradiance rather than the instantaneous field. Since the ensemble average of unresolved field in a correct LES is zero, ensemble average of $\mathcal{L}_e$ is zero as well (see Eq. (2)). Hence, the leading error term in computation of the averaged optical irradiance is of order $\mathcal{L}_e^2/\lambda^2 \sim \xi_0$. As a result, if the ensemble-averaged optical statistics are quantities of interest in an aero-optical simulation, their error is of order ξ_0 and not $\sqrt{\xi_0}$. Therefore, it is not required to choose an extremely small ξ for such computations.

5. Numerical example: aero-optical distortion by flow over a cylinder

To test our analysis for a complex flow configuration, we considered turbulent flow over a circular cylinder, and compared the error of the aero-optical computations due to unresolved flow with that predicted by Eq. (26).

LES of 3D flow over cylinder at $Re = 3900$ and $M = 0.4$ was performed. Fig. 2 shows the computational grid in x-y plane near the cylinder together with a schematic of the optical beam. The computational domain extends to about 18 diameters (D) around the cylinder and the spanwise depth of the domain is πD. The mesh size is $288 \times 200 \times 48$ in wall normal, azimuthal and spanwise directions respectively. The computer code developed by Nagarajan et al. [19] which uses 6th order padé discretization was used for the flow computations. These computations have been validated against previous numerical and experimental studies [3]. 800 snapshots of the flow corresponding from 14 shedding cycles were used for aero-optical computations.

According to Eq. (2), wavefront distortions are computed for an optical beam with diameter of $0.3D$. The beam path starts from the surface of the cylinder and makes an angle of 17° with the direction of downstream mean flow (see Fig. 2). The depth of the turbulent region, Δz, is assumed to be $10D$ in this computation. Using Fourier optics method [20] the far-field optical intensity is computed. The optical wavelength, λ, is assumed to be equal to $5 \times 10^{-6}D$ and the beam was assumed to have a Gaussian profile.

To check the effectiveness of the proposed criterion in predicting the accuracy of aero-optical computations, it is required to compare LES results with that obtained from a well resolved simulation. Therefore, we performed DNS of this flow using a finer grid with size of $576 \times 400 \times 96$ in wall normal, azimuthal and spanwise directions respectively (finer by a factor of 2 in each direction). In addition, instead of relying on RANS, DNS results where used to directly compute the dissipation field (Fig. 3).

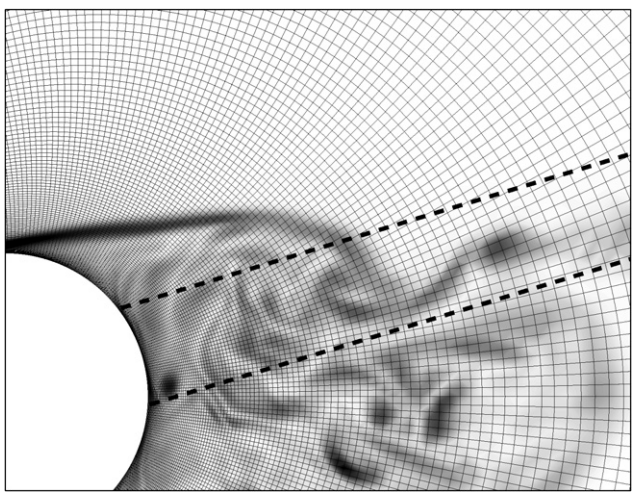

Fig. 2. LES grid in x–y plane. Dashed lines represent the domain of optical propagation. Contours of instantaneous vorticity magnitude (computed by LES) are shown in the background.

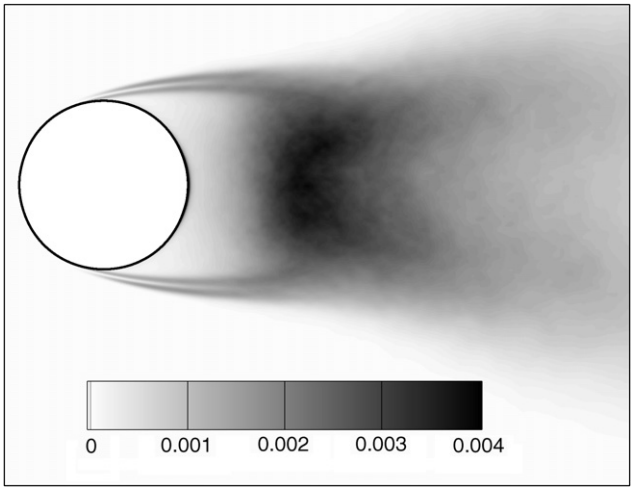

Fig. 3. Dissipation field in the cylinder wake. Values are non-dimensionalized by the speed of sound and cylinder diameter.

Given ϵ from DNS, and l_c from local grid resolution of the coarse grid, Eq. (26) is used to estimate the error of aero-optical computations. In the integration, spatial variation of ensemble-averaged density and speed of sound were ignored due to relatively low Mach number. Assuming $B_p = 8.5$, the error of aero-optical computation based on the LES was calculated to be 12%. In other words it was predicted that, in the aero-optical computation, the energy of the error field. On the other hand the error can be obtained directly by comparing the results of DNS and LES. Fig. 4 shows the mean optical intensity (amplitude squared) profile at the far-field obtained from the two flow simulations. Due to the effect of small flow structures, optical pattern obtained from DNS is more dispersed than that of LES. The average difference between the two plots defined as

$$\frac{\int\int |\,\overline{|U_{\mathrm{DNS}}|^2} - \overline{|U_{\mathrm{LES}}|^2}\,|\,\mathrm{d}x\,\mathrm{d}y}{\int\int \overline{|U_{\mathrm{DNS}}|^2}\mathrm{d}x\,\mathrm{d}y} \tag{27}$$

is computed to be 10% for this case which is close to the estimated value. Eventhough the error measure defined by Eq. (27) is different from the error measure that Eq. (26) predicts, we still obtain about the same value

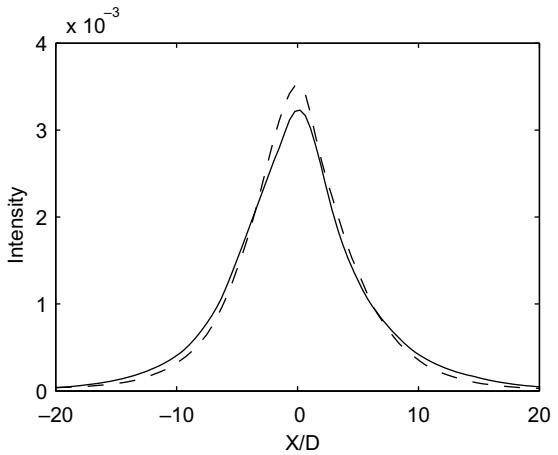

Fig. 4. Ensemble-averaged optical intensity at the far-field distance of $10^5 D$. The x-axis is perpendicular to the beam axis and the averaging is performed in time and homogeneous direction of the flow. Instantaneous results have been tilt-removed before averaging. Intensity values are non-dimensionalized by peak aperture intensity; Solid, DNS; Dashed, LES.

as discussed in Section 4. To have a mathematically consistent test of performance of Eq. (26) we have to compute

$$\frac{\int\int \overline{|U_{\mathrm{DNS}}-U_{\mathrm{LES}}|^2}\,\mathrm{d}x\,\mathrm{d}y}{\int\int \overline{|U_{\mathrm{DNS}}|^2}\,\mathrm{d}x\,\mathrm{d}y}. \tag{28}$$

However, since the two simulations are not instantaneously representing the same flow, it is not reasonable to subtract instantaneous optical results of the two simulations. To remedy this issue, instead of using the LES results for comparison we used optical computations obtained from filtered DNS flow field. A high order low-pass filter with width of twice the grid spacing was used to obtain a coarser(LES) representation of the flow over which optical computation was performed. The electromagnetic fields obtained from DNS was compared to that of filtered DNS and the error based on Eq. (28) was computed to be 13%. Once again, compared to the estimated value of 12%, this result indicates that the proposed analysis can be used to check the adequacy of grid resolution for aero-optical simulations. The difference between the estimated value and the real value of the error is related to several factors including low Reynolds number of the flow, and ignoring spacial variation of $\bar{c}$ and $\bar{n}$.

6. Conclusion

We obtained a criterion to determine the grid resolution required for accurate computation of aero-optical distortions by turbulent flows. Based on this criterion, optical wavelength, depth of the turbulent field, length scale of large flow structures, characteristic Mach number and index of refraction are the governing parameters in determining the required resolution. We observed that the resolution requirement does not scale with Reynolds number for high Reynolds number flows. Also, under practical conditions, this criterion does not impose significant additional cost in a typical LES. This implies that large-eddy simulation with the resolution determined by the proposed criterion can directly capture aero-optical effects of typical flow fields.

Acknowledgments

This work was supported by the Air Force Office of Scientific Research Grant FA9550-06-1-0147. Computations were performed on the NAS facilities at NASA Ames Research Center.

Appendix A. Relationship between $\mathcal{R}_{\mathcal{L}_e}$ and $\mathcal{R}_{n_e}$

In this appendix, the relationship between $\mathcal{R}_{\mathcal{L}_e}$ and $\mathcal{R}_{n_e}$ given by Eq. (8) is derived. By using the ergodic assumption one can write

$$\mathcal{R}_{\mathcal{L}_e}(x,y) \equiv \overline{\mathcal{L}_e(x'+x,y'+y)\mathcal{L}_e(x',y')} \simeq \frac{1}{a}\int_a \mathcal{L}_e(x'+x,y'+y)\mathcal{L}_e(x',y')\mathrm{d}x'\,\mathrm{d}y', \tag{A1}$$

where a is the aperture area whose dimension is much larger than the correlation length scale of $\mathcal{L}_e$. Also, according to its definition, the OPL error due to unresolved flow is

$$\mathcal{L}_e(x,y) = \int_{z=z_0}^{z=z_1} n_e(x,y,z)\mathrm{d}z. \tag{A2}$$

Substituting Eq. (A2) into Eq. (A1) results in

$$\mathcal{R}_{\mathcal{L}_e}(x,y) = \frac{1}{a}\int_{x,y\in a}\left(\int_{z'=z_0}^{z'=z_1} n_e(x'+x,y'+y,z')\mathrm{d}z'\right)\left(\int_{z'=z_0}^{z'=z_1} n_e(x',y',z')\mathrm{d}z'\right)\mathrm{d}x'\,\mathrm{d}y'. \tag{A3}$$

A simple change of variable leads to

$$\mathcal{R}_{\mathcal{L}_e}(x,y) = \frac{1}{a}\int_{x,y\in a}\left(\int_{z=z_0-z'}^{z=z_1-z'} n_e(x'+x,y'+y,z'+z)\mathrm{d}z\right)\left(\int_{z'=z_0}^{z'=z_1} n_e(x',y',z')\mathrm{d}z'\right)\mathrm{d}x'\,\mathrm{d}y'. \tag{A4}$$

By reordering Eq. (A4) we obtain

$$\mathcal{R}_{\mathcal{L}_e}(x,y) = \frac{1}{a}\int_{z'=z_0}^{z'=z_1}\int_{z=z_0-z'}^{z=z_1-z'}\int_{x,y\in a} n_e(x'+x,y'+y,z'+z)n_e(x',y',z')\mathrm{d}x'\,\mathrm{d}y'\,\mathrm{d}z\,\mathrm{d}z'. \tag{A5}$$

In the next step we switch the integration order between z and $z\prime$. To do so we first split the integration domain into two parts:

$$\begin{aligned}\mathcal{R}_{\mathcal{L}_e}(x,y) = &\frac{1}{a}\int_{z'=z_0}^{z'=z_1}\int_{z=0}^{z=z_1-z'}\int_{x,y\in a} n_e(x'+x,y'+y,z'+z)n_e(x',y',z')\mathrm{d}x'\,\mathrm{d}y'\,\mathrm{d}z\,\mathrm{d}z'\\ &+\frac{1}{a}\int_{z'=z_0}^{z'=z_1}\int_{z=z_0-z'}^{z=0}\int_{x,y\in a} n_e(x'+x,y'+y,z'+z)n_e(x',y',z')\mathrm{d}x'\,\mathrm{d}y'\,\mathrm{d}z\,\mathrm{d}z'.\end{aligned} \tag{A6}$$

By switching the order of integration we obtain

$$\begin{aligned}\mathcal{R}_{\mathcal{L}_e}(x,y) = &\frac{1}{a}\int_{z=0}^{z'=\Delta z}\int_{z'=z_0}^{z'=z_1-z}\int_{x,y\in a} n_e(x'+x,y'+y,z'+z)n_e(x',y',z')\mathrm{d}x'\,\mathrm{d}y'\,\mathrm{d}z\,\mathrm{d}z'\\ &+\frac{1}{a}\int_{z=-\Delta z}^{z=0}\int_{z'=z_0-z}^{z'=z_1}\int_{x,y\in a} n_e(x'+x,y'+y,z'+z)n_e(x',y',z')\mathrm{d}x'\,\mathrm{d}y'\,\mathrm{d}z\,\mathrm{d}z',\end{aligned} \tag{A7}$$

where $\Delta z = z_1 - z_0$. Now the integrations over x, y and $z\prime$ can be rewritten in terms of correlations of n_e

$$\begin{aligned}\mathcal{R}_{\mathcal{L}_e}(x,y) &= \int_{z=0}^{z=\Delta z}(z_1 - z - z_0)\mathcal{R}_{n_e}(x,y,z)\mathrm{d}z + \int_{z=-\Delta z}^{z=0}(z_1 + z - z_0)\mathcal{R}_{n_e}(x,y,z)\mathrm{d}z\\ &= \int_{z=-\Delta z}^{z=\Delta z}(\Delta z - |\,z\,|)\mathcal{R}_{n_e}(x,y,z)\mathrm{d}z\end{aligned} \tag{A8}$$

Assuming that the correlation length scale of the unresolved refractive index field n_e is much smaller than depth of turbulence, Δz, $\mathcal{R}_{n_e}$ for fixed x and y will vanish much faster than $\Delta z - |\,z\,|$. Hence, we can assume $\Delta z - |\,z\,| \sim \Delta z$ in the interval of non-zero $\mathcal{R}_{n_e}$. As a result Eq. (A8) can be approximated by

$$\mathcal{R}_{\mathcal{L}_e}(x,y) \simeq \Delta z\int_{z=-\infty}^{z=+\infty}\mathcal{R}_{n_e}(x,y,z)\mathrm{d}z \tag{A9}$$

References

[1] G.W. Sutton, Aero-optical foundations and applications, AIAA Journal 23 (1985) 1525–1537.
[2] M.I. Jones, E.E. Bender, CFD-based computer simulation of optical turbulence through aircraft flowfields and wakes, AIAA Paper 2001-2798.
[3] A. Mani, M. Wang, P. Moin, Computational study of aero-optical distortion by turbulent wake, AIAA Paper 2005-4655.
[4] E. Tromeur, E. Garnier, P. Sagaut, C. Basdevant, Large eddy simulations of aero-optical effects in a turbulent boundary layer, Journal of Turbulence 4 (005) (2003).
[5] A. Mani, M. Wang, P. Moin, Statistical description of the free-space propagation of highly aberrated optical beams, Journal of Optical Society of America A 23 (2006) 3027–3035.
[6] P.E. Dimotakis, H.J. Catrakis, D.C. Fourguette, Flow structure and optical beam propagation in high-Reynolds number gas-phase shear layer and jets, Journal of Fluid Mechanics 433 (2001) 105–134.
[7] E.J. Jumper, E.J. Fitzgerald, Recent advances in aero-optics, Progress in Aerospace Sciences 37 (2001) 299–339.
[8] M.R. Baxter, C.R. Truman, B.S. Masson, Predicting the optical quality of supersonic shear layers, AIAA Paper 88-2771.
[9] R. Smith, C. Truman, Prediction of optical phase degradation using a turbulent transport equation for the variance of index-of-refraction fluctuations, AIAA Paper 90-0250.
[10] C.R. Truman, The influence of turbulent structure on optical phase distortion through turbulent shear flows, AIAA Paper 92-2817.
[11] C.R. Truman, M.J. Lee, Effects of organized turbulence structures on the phase distortion in a coherent optical beam propagating through a turbulent shear flow, Physics of Fluids A 2 (1990) 851–857.
[12] N. Sinha, S. Arunajatesan, J.M. Seiner, L.S. Ukeiley, Large-eddy simulations of aero-optic flow fields and control application, AIAA Paper 2004-2448.
[13] R.E. Childs, Prediction and control of turbulent aero-optical distortion using large eddy simulation, AIAA Paper 93-2670.

[14] R. Mittal, P. Moin, Suitability of upwind-biased finite-difference schemes for large-eddy simulation of turbulent flows, AIAA Journal 35 (1997) 1415–1417.
[15] W. Wolf, G.J. Zizzis, The Infrared Handbook, U.S. Office of Naval Research, Dept. of the Navy, (1978) 16–24.
[16] G.K. Batchelor, Pressure fluctuations in isotropic turbulence, Mathematical Proceedings of the Cambridge Philosophical Society 47 (1951) 359–374.
[17] A.S. Monin, A.M. Yaglom, Mechanics of turbulence, in: J.L. Lumley (Ed.), Statistical Fluid Mechanics, vol. 2, The MIT Press, 1975 (Chapter 9).
[18] T. Gotoh, D. Fukayama, Pressure spectrum in homogeneous turbulence, Physical Review Letters 86 (2001) 3775–3778.
[19] S. Nagarajan, S.K. Lele, J.H. Ferziger, A robust high-order compact method for large eddy simulation, Journal of Computational Physics 191 (2003) 392–419.
[20] J.W. Goodman, Introduction to Fourier Optics, McGraw-Hill, 1996.